Journal of Sound and Vibration (2000) **230**(1), 31–43
doi:10.1006/jsvi.1999.2613, available online at http://www.idealibrary.com on IDEAL®

A TRIANGULAR FOURIER *p*-ELEMENT FOR THE ANALYSIS OF MEMBRANE VIBRATIONS

A. HOUMAT

Institute of Mechanical Engineering, University of Tlemcen, Tlemcen 13000, *Algeria*

(*Received* 12 *January* 1999, *and in final form* 14 *June* 1999)

A triangular Fourier *p*-element for the analysis of membrane vibrations is presented. The element's transverse displacement is written in terms of dimensionless area co-ordinates and is described by three linear shape functions plus a variable number of trigonometric shape functions. The three nodal displacements and the amplitudes of the trigonometric functions on the three edges and in the interior of the element, respectively, are used as generalized co-ordinates. Inter-element compatibility is achieved by matching the generalized co-ordinates at the three nodes and the three edges. Results are obtained for a right isosceles triangular and a square membranes and comparisons are made with exact and linear triangular finite element solutions. The results of both membranes confirm that the solutions converge very fast from above to the exact values as the number of trigonometric terms is increased and highly accurate values are obtained with the use of a very few terms. The results also show that the triangular Fourier *p*-element produces a much higher accuracy than the linear triangular finite element with fewer system degrees of freedom.

1. INTRODUCTION

A triangular Fourier *p*-element is formulated in terms of trigonometric hierarchical shape functions and is applied to membrane vibrations. There are a number of features of the *p*-version of the finite element method also known as the hierarchical finite element method. The most important feature is that a structure may be discretized into elements only once and the number of hierarchical terms in each element is varied. The results can then be obtained to any desired degree of accuracy by simply increasing the number of hierarchical terms.

The hierarchical rectangular finite element of Houmat [1] was formulated in terms of polynomial hierarchical shape functions and was successfully applied to the vibration of membranes whose boundaries are rectangular co-ordinate lines and thus represent the most natural shapes for this type of element.

The polynomial hierarchical finite element method has the drawback that numerical rounding errors associated with floating point arithmetic increase with increasing order of hierarchical function which is basically derived from an

0022-460X/00/060031 + 13 $35.00/0

orthogonal polynomial [2]. This limits the use of the method for high-frequency analysis.

A more promising recent method is the Fourier *p*-version of the finite element method or the trigonometric hierarchical finite element method. In this method, trigonometric shape functions are substituted for the orthogonal polynomial shape functions which are commonly used in the *p*-version of the finite element method. The use of trigonometric shape functions in the hierarchical finite element method is not new. Houmat [3] formulated a hierarchical rectangular finite element in terms of quintic polynomial shape functions plus trigonometric sine shape functions and successfully applied it to the analysis of thin plate vibrations. Besin and Nicholas [4] used only trigonometric sine shape functions and analyzed the same problem. Bardell *et al.* [5] proposed the use of mixed Hermite cubic polynomial shape functions and trigonometric shape functions for the vibration analysis of coplanar sandwich panels. Leung and Chan [6] recommended the use of mixed polynomial and trigonometric shape functions. A comprehensive review of methods applicable to the high-frequency prediction of structures has been compiled by Langley and Bardell [7].

The Fourier *p*-version of the finite element method has been limited currently to rectangular domains. This paper is intended to show the applicability of the method to a triangular domain. In the triangular Fourier *p*-element presented in this paper, the membrane transverse displacement is described by three linear shape functions plus a variable number of trigonometric shape functions. The linear shape functions are used to define the three element nodal displacements and the trigonometric shape functions are used to provide additional freedom to the three edges and the interior of the element. The three nodal displacements and the amplitudes of the trigonometric shape functions on the three edges and in the interior of the element are used as generalized co-ordinates. Inter-element compatibility is achieved by matching the generalized co-ordinates at the element three nodes and three edges. The potential and kinetic energy expressions of membrane undamped free vibrations are used in conjunction with Lagrange equations to develop the equations of motion. A Gaussian quadrature technique is used to evaluate the element stiffness and mass matrices.

Results of frequency calculations using the triangular Fourier *p*-element are given for a right isosceles triangular membrane to show the manner of convergence of the solutions and the way in which the performance of the element compares with that of the linear triangular finite element on a d.o.f. basis. Results are also given for a square membrane to show the applicability of the element to membranes of polygonal shape. The two examples were chosen because exact solutions were available in the literature for comparison.

2. FORMULATION

A triangular membrane element is shown in Figure 1. Also shown in the figure are the dimensionless area co-ordinates ξ_1, ξ_2, and $\xi_3 (=1-\xi_1-\xi_2)$ and their values on the three nodes and the three edges (a list of notation is given in Appendix A).

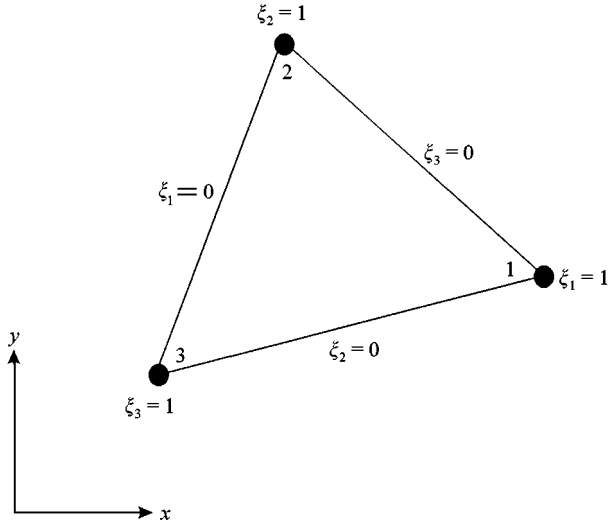

Figure 1. The element co-ordinates.

The expressions for the potential energy U and the kinetic T of the triangular membrane element have the forms

$$U = \frac{S}{4A} \int_A \left[\left(\sum_{l=1}^{3} a_l \frac{\partial w}{\partial \xi_l} \right)^2 + \left(\sum_{l=1}^{3} b_l \frac{\partial w}{\partial \xi_l} \right)^2 \right] \mathrm{d}A, \tag{1}$$

$$T = \rho A \int_A (\dot{w})^2 \, \mathrm{d}A, \tag{2}$$

where the dot denotes differentiation with respect to time, and the parameters a_l and b_l are defined in terms of the three nodal x and y co-ordinates as

$$a_1 = x_3 - x_2, \qquad a_2 = x_1 - x_3, \qquad a_3 = x_2 - x_1, \tag{3–5}$$

$$b_1 = y_2 - y_3, \qquad b_2 = y_3 - y_1, \qquad b_3 = y_1 - y_2. \tag{6–8}$$

The transverse displacement w in this element is expressed as

$$w(\xi_1, \xi_2, \xi_3, t) = \sum_{n=1}^{N} f_n(\xi_1, \xi_2, \xi_3) \, w_n(t), \tag{9}$$

where w_n are generalized co-ordinates and f_n are the following shape functions:

$$f_1 = \xi_1, \qquad f_2 = \xi_2, \qquad f_3 = \xi_3, \tag{10–12}$$

$$f_{n1} = \xi_2 \sin i\pi\xi_1, \qquad f_{n2} = \xi_1 \sin j\pi\xi_2, \qquad f_{n3} = \xi_3 \sin j\pi\xi_2, \tag{13–15}$$

$$f_{n4} = \xi_2 \sin k\pi\xi_3, \qquad f_{n5} = \xi_3 \sin i\pi\xi_1, \qquad f_{n6} = \xi_1 \sin k\pi\xi_3, \tag{16–18}$$

$$f_{n7} = \xi_3 \sin i\pi\xi_1 \sin j\pi\xi_2, \qquad f_{n8} = \xi_1 \sin j\pi\xi_2 \sin k\pi\xi_3, \qquad f_{n9} = \xi_2 \sin i\pi\xi_1 \sin k\pi\xi_3, \tag{19–21}$$

where

$$i, j, k = 1, 2, \ldots, p \tag{22}$$

and p is the number of trigonometric terms used along each direction of the three area co-ordinates.

The indices are defined as

$$n1 = 3 + i, \qquad n2 = 3 + p + j, \qquad n3 = 3 + 2p + j, \tag{23–25}$$

$$n4 = 3 + 3p + k, \qquad n5 = 3 + 4p + i, \qquad n6 = 3 + 5p + k, \tag{26–28}$$

$$n7 = 3 + 6p + (i - 1)\,p + j, \tag{29}$$

$$n8 = 3 + 6p + p^2 + (j - 1)\,p + k, \tag{30}$$

$$n9 = 3 + 6p + 2p^2 + (i - 1)p + k. \tag{31}$$

The assumed displacement shape functions are divided into three sets. The first set consists of shape functions which define the element three nodal displacements. The second set consists of shape functions which give additional freedom to the element's three edges. The third set consists of shape functions which give additional freedom to the interior of the element.

The hierarchical functions $f_{n1}, f_{n2}, \ldots, f_{n9}$ possess zero value at the three nodes. This feature is highly significant since these functions only provide additional freedom to the three edges and the interior of the element and do not influence the three nodal d.o.f. The hierarchical functions f_{n1} and f_{n2} give additional freedom to the edge defined by the nodes 1 and 2, the hierarchical functions f_{n3} and f_{n4} give additional freedom to the edge defined by the nodes 2 and 3, and the hierarchical functions f_{n5} and f_{n6} give additional freedom to the edge defined by the nodes 1 and 3. The hierarchical functions f_{n7}, f_{n8}, and f_{n9} give additional freedom to the interior of the element. Plots of the first six hierarchical functions $f_{n1} = \xi_2 \sin i\pi\xi_1$ ($i = 1, 2, \ldots, 6$) and the first nine hierarchical functions $f_{n7} = \xi_3 \sin i\pi\xi_1 \sin j\pi\xi_2$ (i, $j = 1, 2, 3$) are given, respectively in Tables 1 and 2.

The vector of generalized co-ordinates $\mathbf{w}(t)$ is

$$\mathbf{w}(t) = \{w_1, w_2, w_3, w_{n1}, w_{n2}, w_{n3}, w_{n4}, w_{n5}, w_{n6}, w_{n7}, w_{n8}, w_{n9}\}^{\mathrm{T}}. \tag{32}$$

The co-ordinates w_1, w_2 and w_3 are the element's three nodal displacements. The co-ordinates w_{n1}, w_{n2}, w_{n3}, w_{n4}, w_{n5}, and w_{n6} are the amplitudes of the hierarchical

TABLE 1

The first six hierarchical functions $f_{n1} = \xi_2 \sin i\pi\xi_1$ $(i = 1, 2, \ldots, 6)$

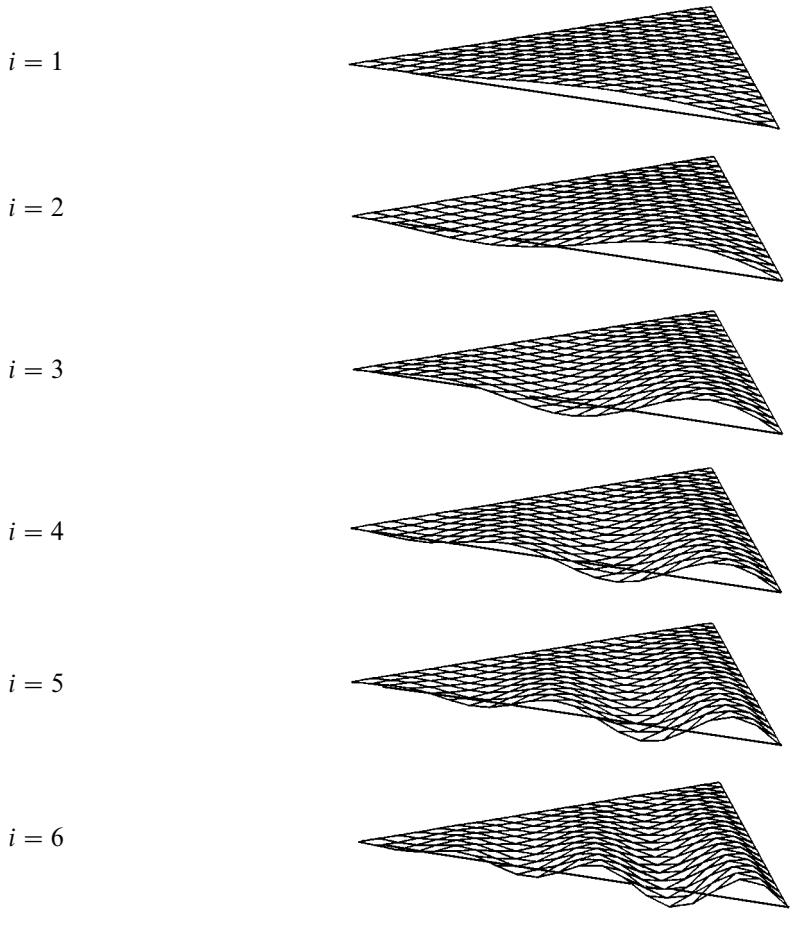

functions on the element's three edges. The co-ordinates w_{n7}, w_{n8}, and w_{n9} are the amplitudes of the hierarchical functions in the interior of the element. The element's generalized co-ordinates are shown in Figure 2.

The equations of motion are determined using the following known Lagrange equations:

$$\frac{\partial U}{\partial w_n} + \frac{\mathrm{d}}{\mathrm{d}t}\left(\frac{\partial T}{\partial \dot{w}_n}\right) = 0. \tag{33}$$

Assuming that the motion is harmonic and inserting the expression for the assumed displacement field (equation (9)) into the element potential and kinetic energy (equations (1) and (2)) then into Lagrange equations (equations (33)) yields the

TABLE 2

The first nine hierarchical functions $f_{n7} = \xi_3 \sin i\pi\xi_1 \sin j\pi\xi_2$ $(i, j = 1, 2, 3)$

$i = j = 1$	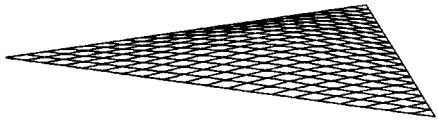
$i = 1, j = 2$	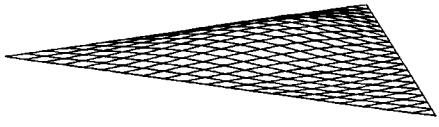
$i = 1, j = 3$	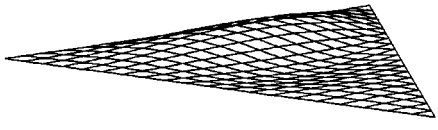
$i = 2, j = 1$	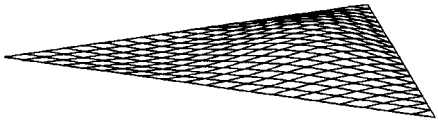
$i = j = 2$	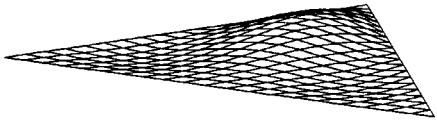
$i = 2, j = 3$	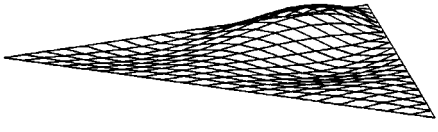
$i = 3, j = 1$	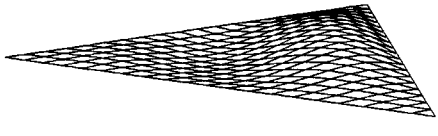
$i = 3, j = 2$	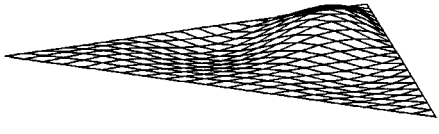
$i = j = 3$	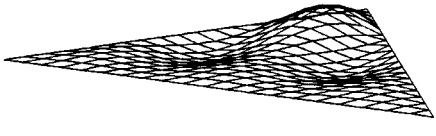

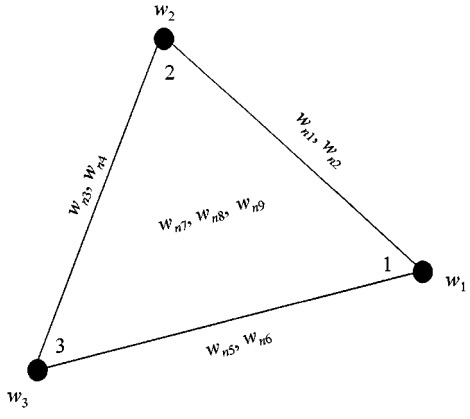

Figure 2. The element generalized co-ordinates.

equation for undamped free vibration which are

$$\sum_{m=1}^{N} [K_{mn} - \omega^2 M_{mn}] w_n = \mathbf{0}, \quad n = 1, 2, \ldots, N. \tag{34}$$

The coefficients of the element stiffness and mass matrices are expressed as

$$K_{mn} = \frac{S}{2A} \sum_{\alpha=1}^{3} \sum_{\beta=1}^{3} (a_\alpha a_\beta + b_\alpha b_\beta) I_{m,n}^{\alpha,\beta}, \qquad M_{mn} = 2\rho A J_{m,n}. \tag{35, 36}$$

The order of the element stiffness and mass matrices is

$$N = 3 + 6p + 3p^2. \tag{37}$$

The integrals are defined as

$$I_{m,n}^{\alpha,\beta} = \int_A \frac{\partial f_m}{\partial \xi_\alpha} \frac{\partial f_n}{\partial \xi_\beta} \, \mathrm{d}A, \qquad J_{m,n} = \int_A f_m f_n \, \mathrm{d}A. \tag{38, 39}$$

The above integrals can be put into the following form:

$$I = \int_0^1 \int_0^{1-\xi_2} g(\xi_1, \xi_2) \, \mathrm{d}\xi_1 \, \mathrm{d}\xi_2. \tag{40}$$

The above integral can be evaluated exactly by using symbolic computing which is available through a number of commercial packages [8]. For low order elements ($p \leqslant 6$), the above integral can be evaluated numerically using Gaussian quadrature

as follows:

$$I = \sum_{r=1}^{R} \sum_{s=1}^{R} u_r u_s g(\xi_{1r}, \xi_{2s}), \tag{41}$$

where

$$u_r = v_r/2, \qquad \xi_{1r} = \tfrac{1}{2}(1 + \eta_r), \tag{42, 43}$$

$$u_s = \tfrac{1}{2}(1 - \xi_{1r})v_s, \qquad \xi_{2s} = \tfrac{1}{2}(1 - \xi_{1r})(1 + \eta_s), \tag{44, 45}$$

and η_r and v_r are, respectively, the abscissas and weight of the integration point r, and R is the number of integration points which are used to integrate a one-dimensional function h in the interval $(-1, 1)$ using Gaussian quadrature as follows:

$$\int_{-1}^{1} h(\eta)\, \mathrm{d}\eta = \sum_{r=1}^{R} h(\eta_r) v_r. \tag{46}$$

Particular boundary conditions can be specified on the three nodes and the three edges of each element. For each specified boundary condition, the corresponding row and column must be deleted from the system stiffness and mass matrices. The resulting generalized eigenvalue problem can then be solved using any known technique.

Inter-element compatibility is achieved by assuming that the generalized co-ordinates w_{n1}, w_{n2}, w_{n3}, w_{n4}, w_{n5}, and w_{n6} on the element's three edges are associated with fictitious nodes $n1$, $n2$, $n3$, $n4$, $n5$, and $n6$, respectively, and so numbers are assigned to them in the same way as the three real nodes. The processes of assembly and application of boundary conditions will therefore be similar to their counterparts in the standard finite element method and so the known techniques used in the finite element method become applicable. This process has been previously used by Houmat [1].

3. RESULTS

Results of the application of the triangular Fourier p-element to the calculation of the frequency parameter Ω are first found for a simply supported right isosceles triangular membrane with orthogonal sides lengths equal to 1.

Exact solutions are available in the literature for this membrane [9]. In order to see the manner of convergence of the solutions, the membrane is discretized into one triangular Fourier p-element and the number of trigonometric terms p is varied. Results for the 10 lowest modes are shown in Table 3 along with the exact solutions. Table 3 clearly shows that a very fast convergence from above to the exact values occurs as the number of trigonometric terms in increased from two to five and the values for $p = 5$ are in excellent agreement with the exact ones. In Table 3, there is an obvious typographical error in reference [9]. The exact value for the 10th frequency parameter was given as 19·120 when it should have been 19·110. In fact, 19·110 was found to be the value converged upon by the triangular Fourier p-element by using five or more trigonometric terms.

TABLE 3

Convergence of the 10 *lowest frequency parameters* Ω *for the right isosceles triangular membrane* (*the whole membrane is discretized into one triangular Fourier p-element*) *as a function of the number of trigonometric terms p*

p	1	2	3	4	5	6	7	8	9	10
2	7·0343	9·9643	11·361	12·995	14·756	16·304	18·743	19·336	21·016	22·292
3	7·0252	9·9349	11·328	12·972	14·076	15·739	16·076	17·052	18·834	19·404
4	7·0248	9·9346	11·327	12·953	14·050	15·709	16·022	16·928	18·353	19·123
5	7·0248	9·9346	11·327	12·953	14·050	15·708	16·019	16·918	18·318	19·110
Exact	7·0248	9·9346	11·327	12·953	14·050	15·708	16·019	16·918	18·318	19·110

TABLE 4

Comparison of the 10 *lowest frequency parameters* Ω *for the right isosceles triangular membrane. Numbers in parenthesis denote the numbers of system d.o.f.*

Type of element		1	2	3	4	5	6	7	8	9	10
Triangular Fourier *p*-element	(12)	7·0343	9·9643	11·361	12·995	14·756	16·304	18·743	19·336	21·016	22·292
Linear triangular element	(15)	7·3239	10·8968	12·522	14·958	16·813	18·504	19·401	21·390	23·350	23·557
Triangular Fourier *p*-element	(27)	7·0252	9·9349	11·328	12·972	14·076	15·739	16·076	17·052	18·834	19·404
Linear triangular element	(36)	7·1725	10·4124	11·938	13·958	15·493	17·205	17·862	19·374	21·368	22·080
Triangular Fourier *p*-element	(48)	7·0248	9·9346	11·327	12·953	14·050	15·709	16·022	16·928	18·353	19·123
Linear triangular element	(55)	7·1277	10·2673	11·758	13·651	15·069	16·783	17·307	18·641	20·529	21·229
Triangular Fourier *p*-element	(75)	7·0248	9·9346	11·327	12·953	14·050	15·708	16·019	16·918	18·318	19·110
Linear triangular element	(78)	7·0687	10·1623	11·672	13·392	14·768	16·422	16·980	18·077	20·058	20·698
Exact		7·0248	9·9346	11·327	12·953	14·050	15·708	16·019	16·918	18·318	19·110

The performance of the triangular Fourier p-element with that of the linear triangular finite element on a d.o.f. basis is also investigated. The linear triangular finite element represents the special case of the triangular Fourier p-element when no trigonometric terms are used ($p = 0$). Results for the 10 lowest modes of the right isosceles triangular membrane are shown in Table 4 along with the exact solutions and the solutions from the linear triangular finite element. The number of trigonometric terms p used in the triangular Fourier p-element are 2, 3, 4, and 5 and the corresponding numbers of system d.o.f. are 12, 27, 48, and 75 respectively. The linear triangular finite element solutions were obtained by discretizing the triangular membrane into 49, 100, 144, and 196 elements and the corresponding numbers of system d.o.f. are 15, 36, 55, and 78 respectively. Table 4 clearly shows that the triangular Fourier p-element solutions are largely more accurate than the linear triangular finite element ones despite the use of fewer system d.o.f.

In order to show the applicability of the triangular Fourier p-element to membranes of polygonal shape, a simply supported square membrane of side length equal to 2 was considered. Exact solutions are available in the literature for this membrane [10]. Because of symmetry in geometry and in boundary conditions and by centering the co-ordinate system it is necessary to consider only one-quarter. The solution for the entire membrane may be obtained from the solution for one-quarter with three different sets of boundary conditions on the symmetry lines. The solutions for the one-quarter will therefore fall into three groups: symmetric–symmetric modes, symmetric–antisymmetric modes, and antisymmetric–antisymmetric modes. In order to see the manner of convergence of the solutions, one-quarter of the membrane is discretized into two identical triangular Fourier p-elements and an equal number of trigonometric terms p is used in both elements. Results for the 10 lowest modes are shown in Table 5 along with the exact solutions. Modes 1, 4, 7, and 10 are symmetric–symmetric modes, modes 2, 5, 6, and 9 are symmetric–antisymmetric modes, and modes 3 and 8 are antisymmetric–antisymmetric modes. Table 5 clearly shows that a very fast convergence from above to the exact values occurs as the number of trigonometric terms p in each element is increased from two to five and the solutions for $p = 5$ are in excellent agreement with the exact ones.

4. CONCLUSION

A triangular Fourier p-element for membrane vibrations has been presented. The element displacement field is written in terms of three dimensionless area co-ordinates and is described by three linear shape functions plus a variable number of trigonometric shape functions. The three nodal displacements and the amplitudes of the trigonometric shape functions on the three edges and in the interior of the element are used as generalized co-ordinates. Inter-element compatibility is achieved by matching the generalized co-ordinates at the three nodes and the three edges.

Results of a right isosceles triangular membrane have shown that the triangular Fourier p-element solutions converge very fast from above to the exact values as the

TABLE 5

Convergence of the 10 *lowest frequency parameters* Ω *for the square membrane* (*one quarter is discretized into two identical triangular Fourier p-elements*) *as a function of the number of trigonometric terms p in each element*

p	1	2	3	4	5	6	7	8	9	10
2	2·22147	3·51268	4·44512	4·96835	5·66990	6·48333	6·68426	7·03430	7·92269	8·02254
3	2·22144	3·51242	4·44298	4·96732	5·66381	6·47682	6·66449	7·02485	7·85454	8·00978
4	2·22144	3·51241	4·44288	4·96729	5·66359	6·47656	6·66433	7·02482	7·85400	8·00953
5	2·22144	3·51241	4·44288	4·96729	5·66359	6·47656	6·66432	7·02481	7·85398	8·00952
Exact	2·22144	3·51241	4·44288	4·96729	5·66359	6·47656	6·66432	7·02481	7·85398	8·00952

number of trigonometric terms in increased and highly accurate values are obtained with the use of a very few terms. Comparisons of the results of the triangular membrane on a d.o.f. basis have shown that the triangular Fourier *p*-element yields a much higher accuracy than the linear triangular finite element with fewer system d.o.f. The applicability of the triangular Fourier *p*-element to membranes of polygonal shape has been demonstrated by considering a square membrane discretized into two identical triangular Fourier *p*-elements and highly accurate values have been obtained with the use of a very few trigonometric terms in each element.

REFERENCES

1. A. Houmat 1997 *Journal of Sound and Vibration* **201**, 465–472. Hierarchical finite element analysis of the vibration of membranes.
2. L. J. West, N. S. Bardell, J. M. Dunsdon and P. M. Loasby 1997 *Proceedings of the Sixth International Conference on Recent Advances in Structural Dynamics, Southampton*. Some limitations associated with the use of *K*-orthogonal polynomials in hierarchical versions of the finite element method.
3. A. Houmat 1997 *Journal of Sound and Vibration* **206**, 201–215. An alternative hierarchical finite element formulation applied to plate vibrations.
4. O. Beslin and J. Nicolas 1997 *Journal of Sound and Vibration* **202**, 633–655. A hierarchical functions set for predicting very high order plate bending modes.
5. N. S. Bardell, J. M. Dunsdon and R. S. Langley 1997 *Composite Structures* **38**, 463–475. Free vibration of coplanar sandwich panels.
6. A. Y. T. Leung and J. K. W. Chan 1998 *Journal of Sound and Vibration* **212**, 179–185. Fourier *p*-element for the analysis of beams and plates.
7. R. S. Langley and N. S. Bardell 1998 *The Aeronautical Journal* **102**, 287–297. A review of current analysis capabilities applicable to the high frequency vibration prediction of aerospace structures.
8. N. S. Bardell 1989 *International Journal for Numerical Methods in Engineering* **28**, 1181–1204. The application of symbolic computing to the hierarchical finite element method.
9. M. G. Milsted and J. R. Hutchinson 1974 *Journal of Sound and Vibration* **32**, 327–346. Use of trigonometric terms in the finite element method with application to vibrating membranes.
10. J. R. Hutchinson 1985 *Boundary Elements VII—Proceedings of the Seventh International Conference, Como, Italy*. An alternative BEM formulation applied to membrane vibrations.

APPENDIX A: NOMENCLATURE

ξ_1, ξ_2, ξ_3	dimensionless area co-ordinates
x, y	Cartesian co-ordinates
A	element surface area
ρ	membrane surface density
S	membrane surface tension
t	time
w	membrane transverse displacement
U	element potential energy
T	element kinetic energy

K_{mn}	coefficients of the element stiffness matrix
M_{mn}	coefficients of the element mass matrix
$\mathbf{w}$	vector of generalized co-ordinates
p	number of trigonometric terms
N	order of element stiffness and mass matrices
ω	natural frequency
Ω	$= \omega\sqrt{\rho/S}$, frequency parameter